First-order reversal curves (FORCs) of nano-engineered 3D Co-Fe structures

Mohanad Al Mamoori, Christian Schröder, Lukas Keller, Michael Huth, and Jens Müller

COLLECTIONS

Paper published as part of the special topic on 64th Annual Conference on Magnetism and Magnetic MaterialsMMM2020, 64th Annual Conference on Magnetism and Magnetic MaterialsMMM2020, 64th Annual Conference on Magnetism and Magnetic MaterialsMMM2020, 64th Annual Conference on Magnetism and Magnetic MaterialsMMM2020, 64th Annual Conference on Magnetism and Magnetic MaterialsMMM2020 and 64th Annual Conference on Magnetism and Magnetic MaterialsMMM2020

View Online   Export Citation   CrossMark

ARTICLES YOU MAY BE INTERESTED IN

What does a first-order reversal curve diagram really mean? A study case: Array of ferromagnetic nanowires
Journal of Applied Physics **113**, 043928 (2013); https://doi.org/10.1063/1.4789613

First order reversal curves (FORC) analysis of individual magnetic nanostructures using micro-Hall magnetometry
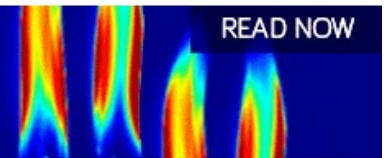Review of Scientific Instruments **87**, 113907 (2016); https://doi.org/10.1063/1.4967940

Launching a new dimension with 3D magnetic nanostructures
APL Materials **8**, 010701 (2020); https://doi.org/10.1063/1.5134474

First-order reversal curves (FORCs) of nano-engineered 3D Co-Fe structures

Mohanad Al Mamoori,[1,2,a] (iD) Christian Schröder,[3,4] Lukas Keller,[1] Michael Huth,[1] and Jens Müller[1]

AFFILIATIONS

[1] Institute of Physics, Goethe-University Frankfurt, 60438 Frankfurt am Main, Germany
[2] Institute of Materials Science, Technical University of Darmstadt, 64287 Darmstadt, Germany
[3] Institute for Applied Materials Research, Bielefeld University of Applied Science, 33619 Bielefeld, Germany
[4] Faculty of Physics, Bielefeld University, 33501 Bielefeld, Germany

Note: This paper was presented at the 64th Annual Conference on Magnetism and Magnetic Materials.
[a] Electronic mail: AlMamoori@Physik.uni-frankfurt.de

ABSTRACT

In this paper we present first-order reversal curve (FORC) diagrams of ensembles of three-dimensional Co_3Fe nanostructures as 2×2 arrays of nano-cubes and nano-trees. The structures are fabricated and investigated by an advanced platform of focused electron beam induced deposition combined with high-resolution detection of magnetic stray fields using a home-built micro-Hall magnetometer based on an AlGaAs/GaAs heterostructure. The experimental FORC diagrams are compared to macrospin simulations for both geometries at different angles of the externally applied magnetic field. The measured FORC diagrams are in good agreement with the simulated ones and reflect non-uniform magnetization reversal dominated by multi-vortex states within, and strong magnetic coupling between, the building blocks of our nanostructures. Thus, a FORC analysis of small arrays of 3D magnetic nanostructures provides more detailed insights into the mechanisms of magnetization reversal beyond standard major hysteresis loop measurements.

I. INTRODUCTION

Magnetic nanostructures have become key building blocks in many areas of fundamental research in magnetism as well as in nano-technological fabrication of functional applications. Identifying intrinsic magnetic properties as well as the nature of interactions in larger networks is a challenging task that requires both advanced fabrication tools and investigation techniques. Advanced methods to study ferromagnetic hysteresis, like the measurement of first-order reversal curves (FORCs),[1] represent an appropriate tool for investigating processes that take place during the often complex magnetization reversal, which may be inaccessible by measuring a global hysteresis loop. The attractiveness of the FORC method lies in its straightforward application to large ensembles of nanoscale magnets, such as arrays of interacting one- or two-dimensional magnetic nanostructures, see, e.g. Ref. 2–4

Therefore, accessing also three-dimensional (3D) nanomagnetic structures with this method appears as a promising approach

to probing the behaviour of the expected complex magnetization reversal processes. Recently, we have demonstrated the fabrication of building blocks for artificial magnetic lattices, aiming to advance beyond planar arrays toward the creation of 3D nanomagnetic networks, which were investigated experimentally by ultra-sensitive micro-Hall magnetometers and simulated by macro- and micromagnetic approaches.[5,6]

Here, we discuss FORC diagram signatures of these ensembles of 3D Co_3Fe (CoFe) structures as small (2×2) arrays of nano-cubes and nano-trees measured by micro-Hall magnetometry[7] to gain further insights into the observed magnetic reversal processes. Experimental results are compared to simulations based on an idealized theoretical model using single-dipole macrospins (SDMS).

II. EXPERIMENTAL METHODS

The samples consist of metallic bcc Co_3Fe grown as nano-cubes and nano-trees that were directly written on the active area of a

micro-Hall sensor surface using focused electron beam deposition (FEBID). Details about FEBID nano-fabrication of 3D geometries can be found elsewhere.[6,8–10] The perpendicular stray field $\langle B_z \rangle$ averaged over the active area of the Hall-cross, which is directly linked to the sample magnetization,[11] is measured by detecting the generated Hall voltage V_H in the micro-Hall sensor plane (formed by

FIG. 1. (a) SEM image of two $5 \times 5 \ \mu m^2$ Hall crosses with arrays of 2×2 CoFe nano-cubes and nano-trees grown by FEBID directly on the surface. The Hall voltage generated in the sensor plane is directly proportional to the sample magnetization. (b) Schematic drawing of the FORC data acquisition protocol. Calculation of the second-order mixed derivative of the magnetic signal with respect to H_r and H_a results in the FORC distribution.

a high-mobility two-dimensional electron gas at the interface of an AlGaAs/GaAs heterostructure).[12] The large linear Hall-effect background signal is cancelled *in situ* by a differential measurement of an empty reference Hall cross in a so-called gradiometry set-up according to $\Delta V_H = \frac{1}{ne} I < B_z >$, where n is the carrier density and I the applied current.

The FORC data acquisition routine using the electronic readout of the Hall sensor[7] is extended to perform FORC protocols for our 3D CoFe nanostructures. The FORC acquisition protocol[1,13] is depicted in Fig. 1(b). First, the sample is saturated in a large positive applied magnetic field H_{sat}. Second, the magnetic field is ramped down to the reversal field H_r. The first FORC is obtained when the applied field H_a is increased up to saturation. This process is repeated for many values of approximately evenly spaced H_r, from H_r to H_{sat}. The FORC distribution is conveniently represented by a rotated coordinate system, the horizontal axis (representing the switching fields) given by $H_c = (H_a - H_r)/2$ and the vertical axis (representing the interaction fields) given by $H_u = (H_a + H_r)/2$. To obtain the FORC distribution, the raw magnetization data are then further processed with a suitable code (FORCinel)[14] using smoothing factors ranging from 6 to 10.

III. RESULTS AND DISCUSSION

FORC distributions provide additional information to that revealed by global hysteresis loops, thereby allowing a better understanding of the mechanisms of magnetization reversal through the analysis of coercive and interaction field distributions. Many magnetic structures, such as nanoparticles and -dots,[15] nanowires[16] or GMR devices,[17] have been investigated using this method. In the following, we discuss FORC diagrams of our 3D CoFe nano-cubes and nano-trees, that have been investigated by global hysteresis loop measurements in Refs. 5 and 6. Here, FORC data from micro-Hall magnetometry measurements have been obtained at a maximum saturation field $\mu_0 H_{sat} = 150$ mT at $T = 25$ K, with a sweep rate of 10 mT/min and reversal field steps $\Delta \mu_0 H_r = 2$ mT. FORC distributions were calculated from the raw data on an equidistant grid using the FORCinel code.[14]

Figure 2(a) shows the experimental FORC diagram for an array of 2×2 CoFe nano-cubes at $\theta = 0$, *i.e.* the applied field perpendicular to the sensor plane and parallel to the anisotropy axis of the nano-cube stems. The inset shows corresponding raw FORCs for the measured structures. As reported before,[5,6] the large magnetic volume of the nano-cubes consisting of many connected bistable rods leads to step-like switching events seen in the global hysteresis loop, where the magnetisation reversal likely develops by inhomogeneous multi-vortex states nucleating, propagating and annihilating through the individual building blocks as well as the three- and four-leg joints. It should be mentioned that the detailed account of multi-vortex FORC signatures was firstly reported in geologic materials.[18] In our FORC diagram, this results in complex signatures in the H_u-H_c plane accompanied by circular loops of intensities forming around the central ridge. The first dominant signature is a strong and broad peak in the FORC diagram with a slight offset to the $H_u = 0$ axis and overlapping with peak-like features lined up vertically. This central peak is caused by the magnetization switching ($\mu_0 H_c^{FORC} = 22.5$ mT at $\mu_0 H_u = 0$) of the stems that are aligned parallel to the applied
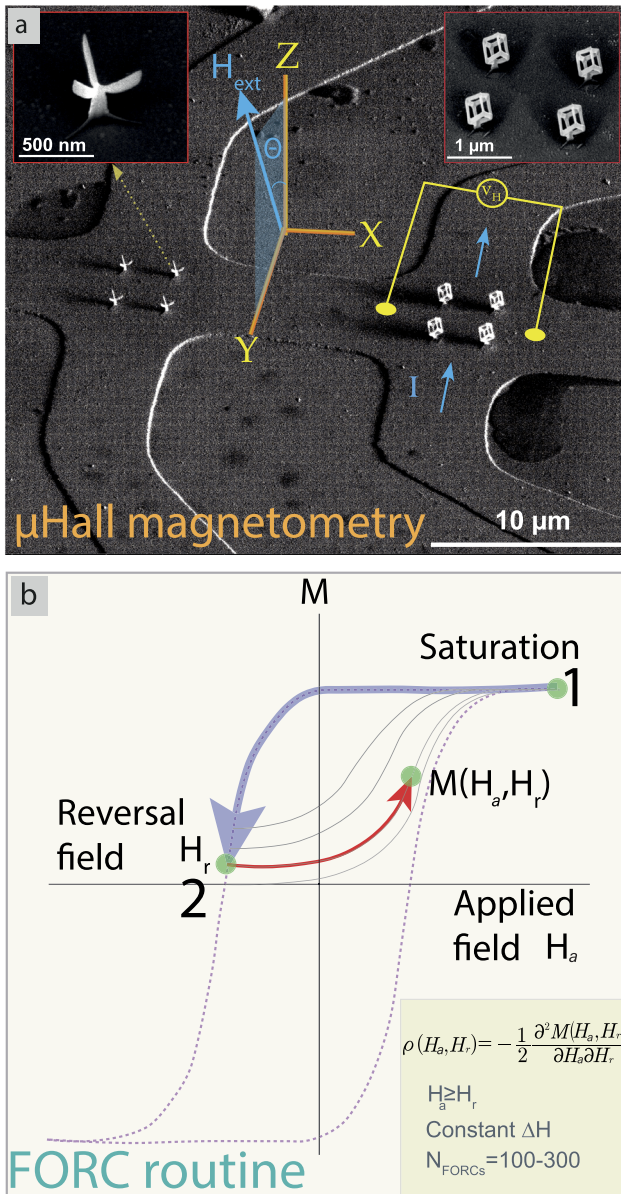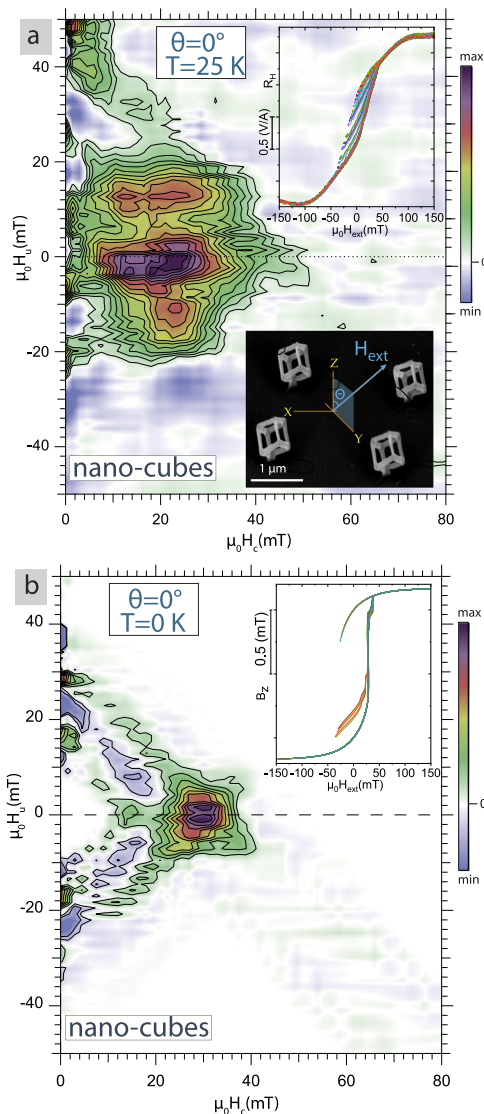
FIG. 2. (a) Experimental FORC distribution of 2 × 2 individual CoFe nano-cubes obtained at a 0° applied field direction (parallel to the stems) at T = 25 K. Upper inset: family of FORCs from which the corresponding contour plot is calculated. Lower inset: scanning electron microscope image of the CoFe nano-cubes. (b) Simulated FORC distribution from macrospin simulations for the corresponding structures.

A quantitative analysis of the interaction fields at the coercivity peak is best illustrated by a vertical profile (not shown here). From the latter, the full width at half maximum (FWHM) is determined to about 33.3 mT.

We compare our experimental FORC diagrams with simulations based on an idealized theoretical model using single-dipole macrospins (SDMS),[11] where one SDMS reflects the magnetic behaviour of an ideal, *i.e.* single-domain, stem or edge. Each SDMS is located at the center of the building block positions. Assuming each building block to represent a prolate spheroid with a homogeneous magnetization allows us to relate their magnetic properties to the Stoner-Wohlfarth model[19] of a particle with uniaxial anisotropy. The SDMS model consists of four SDMS per nano-tree and thirteen SDMS per nano-cube. The SDMS interact via dipole-dipole interaction only. The FORCs of these systems have been calculated for T = 0 by solving the stochastic Landau-Lifshitz equation[11] following essentially the same acquisition protocol as used in the experiment. Since the macrospin model only contains interacting SDMS, all features observed in the simulated FORC diagrams merely correspond to the properties of simple Stoner-Wolfarth[19] particles and the dipole-dipole interactions among them. This means that generally there are fewer features expected in simulated FORC diagrams, which in turn can be used to identify additional features in the experimental FORC diagrams that originate from physical mechanisms beyond the macrospin model.

Figure 2(b) shows the FORC diagram for the nano-cubes calculated from the simulated FORCs shown in the upper inset. Compared to the experimental FORC, essential features on the central ridge can be reproduced, however, with less intensity and more peaked (*i.e.* with a narrower distribution) on the central ridge. The less dominant coercivity peaks at negative and positive $\mu_0 H_u$ values are shifted further away from the reversal side and coincide at $\mu_0 H_u$ = 0 mT, unlike the experiment. The coercivity distribution is peaked at $\mu_0 H_c^{FORC}$ = 29.9 mT comparable to the coercivity from global hysteresis loop measurements. Broadening of the experimental FORC features on the central ridge as well as peaks in the positive and negative $\mu_0 H_u$ are likely attributed to switching of non-uniformly magnetized edges and stems.

Changing the field angle with respect to the stem and edges to θ = 90° (the applied field parallel to the sensor plane and perpendicular to the nano-cube stems) leads to a more complex FORC diagram as shown in Fig. 3. One observes many prominent features distributed in the upper and lower half planes and weaker negative features at different positions. The most pronounced features consisting of circular positive regions are those located on the negative diagonal highlighted by the blue arrow. For example, in simple arrays of Co nanodots,[15] such circular peaks have been attributed to distinct annihilation and nucleation paths. In our case, the occurrence of such circular peaks may be attributed to the nucleation and annihilation of vortex states within the magnetic edges, stems and the vertices of the nano-cubes since they have different anisotropy orientations giving rise to multiple separated peaks in the FORC diagram progressively shifting to higher coercivities. We find the coercivity at θ = 90° approximately peaked at $\mu_0 H_c^{FORC}$ = 48 mT (at $\mu_0 H_u$ = 0), a value higher than for θ = 0° (Fig. 2). This is expected from the anisotropy of the structures and may be explained by the dominating contribution of the stems with inhomogeneous spin texture involving creation and annihilation of magnetic vortices.
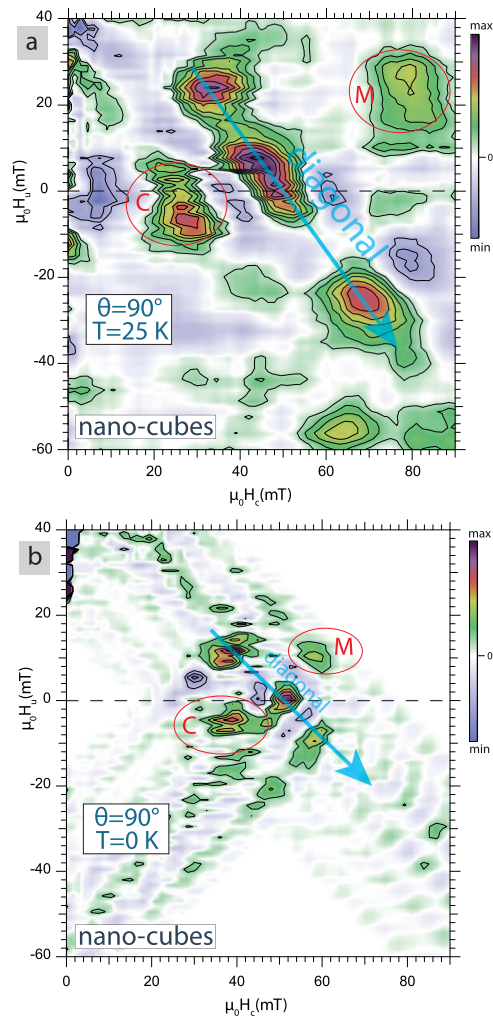
magnetic field, which is approximately equivalent to the coercive field of the global hysteresis loop $\mu_0 H_c^{hyst.}$ = 22.1 mT. The different orientations of the edge elements lead to a distribution of switching fields and hence to a "stretched" central peak in the FORC diagram. It should be noted that the shape of the coercivity distribution likely reflects magnetic vortex nucleation and annihilation. Furthermore, the predominant vertically elongated features (subsidiary overlapping vertical peaks) might be due to vortex nucleation and annihilation field distributions in non-uniformly magnetized edges and interactions between vortices of the same or neighboring edges.

FIG. 3. (a) Experimental FORC distribution of 2 × 2 individual CoFe nano-cubes obtained at a 90° applied field direction (perpendicular to the stems) and at $T = 25$ K. (b) Simulated FORC distribution from macrospin simulations.

The experimental and simulated FORC diagrams obtained for the 2 × 2 nano-tree array are shown in Fig. 4. The experimental FORC diagram is shown in Fig. 4(a) for $\theta = 0°$, where the anisotropy axis of the stems points in the field direction, with the lower inset showing a scanning electron microscope image of the structures. We find that the FORC distribution is dominated by an asymmetric, fish-like positive central area centered along the horizontal axis.
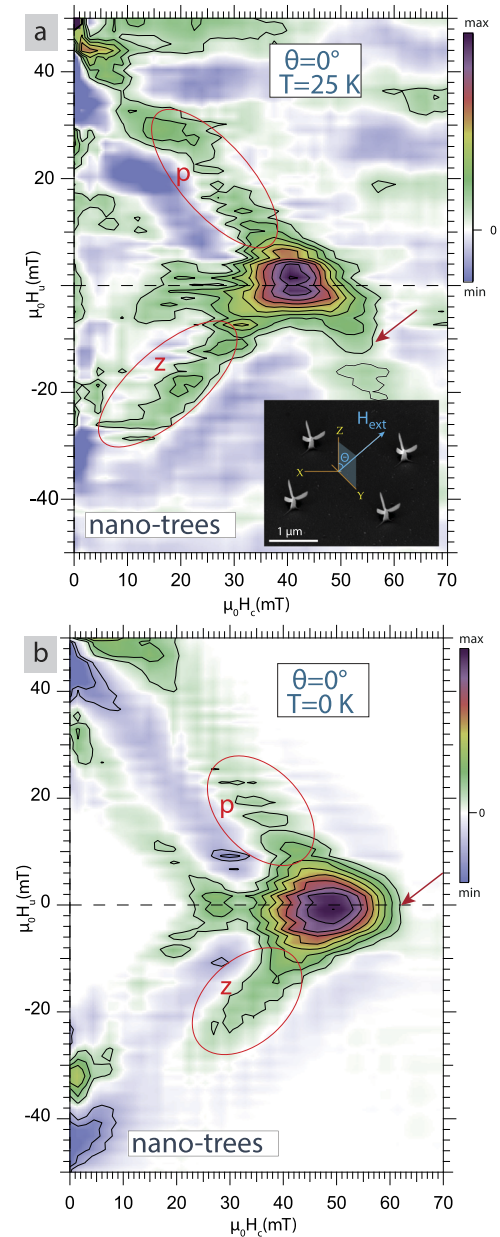

FIG. 4. (a) Experimental FORC distribution of 2 × 2 individual CoFe nano-trees obtained at a 0° applied field direction (parallel to the stems) and at $T = 25$ K. Inset: SEM image of CoFe nano-trees. (b) Simulated FORC distribution from macrospin simulations for the corresponding structures.

Additionally, shape irregularities play a vital role in vortex annihilation and nucleation processes. The magnetization reversal via different intermediate states causes non-deterministic switching events, *i.e.* they do not necessarily occur at the same field in ascending and descending branches of the FORC leading to the observed asymmetric isolated peaks (see the peaks marked C and M). Such behaviour might indicate strong interaction effects (the connected two upper and separated lower peaks of the diagonal reveal a reasonable vertical spread filling the FORC space). The simulated FORC distribution for this selected angle shown in Fig. 3(b) remarkably reveals some essential features, however, with lower peak intensity. The diagonal circular peaks are reproduced, although at different positions. The side circular peaks (C and M) also appear in the simulated FORC diagram. As explained above, the lower intensity and sharper peak structure reflect the properties of interacting idealized Stoner-Wolfarth[19] particles.

There are also weak negative features visible in the FORC space. The central area has a strong peak at $\mu_0 H_c^{\text{FORC}}$ = 40 mT. The horizontal positive distribution of contours reflects a broad coercivity distribution (the horizontal line projection, not shown here, has a Gaussian curve). Switching of the nano-trees develops by inhomogeneous vortex states along the edges and the stems.[5,6] It commences by the edges switching before reversal of the major part of the sample volume, *i.e.* the stems, which are the last to switch causing the sharp step in the major hysteresis loop.[5,6] The low-end of coercivity (highlighted by z-zone) is shifted toward negative $\mu_0 H_u$, while the p-zone is shifted to the positive direction. Such vertical spread is a direct measure of a broad interaction distribution. A vertical profile at the coercivity peak yields a *FWHM* = 11.5 mT, which is a measure of interaction effects both between the building blocks within a nano-tree structure and between neighbouring structures. The simulated FORC diagram is shown in Fig. 4(b). Strikingly, it is in good qualitative and reasonable quantitative agreement with the experiment. The coercivity peak is found at $\mu_0 H_c^{\text{FORC}}$ = 49 mT. The tails (p- and z-zones) are less shifted along the H_u-axis, which is again due to the assumption of idealized single-domain stems and edges in our simulations. In addition, the high coercivity end (red arrow) coincides on the horizontal line (at $\mu_0 H_u$ = 0). The vertical profile (not shown here) reveals a *FWHM* = 12.5 mT, as a measure of the interaction field strength among the magnetic entities which is in good quantitative agreement with the experiment.

IV. CONCLUSIONS

In this paper, we present the first FORC diagrams for FEBID-fabricated 3D CoFe nanostructures grown as stem-mounted nano-cubes and nano-trees directly on top of 5×5 μm^2 Hall crosses of an ultra-sensitive micro-Hall sensor. We have applied the external magnetic field at different angles and complemented the experimental results with simulations based on a theoretical model of single-dipole macrospins (SDMS), which reflect the magnetic behavior of ideal, *i.e.* single-domain building blocks of the nanostructures. The FORC signatures for both geometries have complex coercive field and interaction field distributions. This reflects non-uniform magnetization reversal of the stems and edges dominated by multi-vortex states, and strong magnetic coupling between the magnetic entities. The FORC diagrams calculated from SDMS simulations agree well with the experiments and prove to be a useful characterization tool for the switching dynamics also of structures of this kind. The observations in this study provide an avenue for future research to unveil complex magnetic switching and interaction scenarios of various 3D nanomagnets by adapting the FORC technique to combined FEBID fabrication/micro-Hall magnetometry.

ACKNOWLEDGMENTS

REFERENCES

[1] C. R. Pike, A. P. Roberts, and K. L. Verosub, "Characterizing interactions in fine magnetic particle systems using first order reversal curves," Journal of Applied Physics **85**, 6660–6667 (1999).

[2] D. A. Gilbert, G. T. Zimanyi, R. K. Dumas, M. Winklhofer, A. Gomez, N. Eibagi, J. Vicent, and K. Liu, "Quantitative decoding of interactions in tunable nanomagnet arrays using first order reversal curves," Scientific Reports **4**, 4204 (2014).

[3] D. A. Gilbert, B. B. Maranville, A. L. Balk, B. J. Kirby, P. Fischer, D. T. Pierce, J. Unguris, J. A. Borchers, and K. Liu, "Realization of ground-state artificial skyrmion lattices at room temperature," Nature Communications **6**, 8462 (2015).

[4] R. K. Dumas, C.-P. Li, I. V. Roshchin, I. K. Schuller, and K. Liu, "Magnetic fingerprints of sub-100 nm Fe dots," Physical Review B **75**, 134405 (2007).

[5] M. Al Mamoori, L. Keller, J. Pieper, S. Barth, R. Winkler, H. Plank, J. Müller, and M. Huth, "Magnetic characterization of direct-write free-form building blocks for artificial magnetic 3D lattices," Materials **11**, 289 (2018).

[6] L. Keller, M. K. Al Mamoori, J. Pieper, C. Gspan, I. Stockem, C. Schröder, S. Barth, R. Winkler, H. Plank, M. Pohlit *et al.*, "Direct-write of free-form building blocks for artificial magnetic 3D lattices," Scientific Reports **8**, 6160 (2018).

[7] M. Pohlit, P. Eibisch, M. Akbari, F. Porrati, M. Huth, and J. Müller, "First order reversal curves (FORC) analysis of individual magnetic nanostructures using micro-Hall magnetometry," Review of Scientific Instruments **87**, 113907 (2016).

[8] R. Winkler, B. B. Lewis, J. D. Fowlkes, P. D. Rack, and H. Plank, "High-fidelity 3D-nanoprinting via focused electron beams: Growth fundamentals," ACS Applied Nano Materials **1**, 1014–1027 (2018).

[9] R. Winkler, F.-P. Schmidt, U. Haselmann, J. D. Fowlkes, B. B. Lewis, G. Kothleitner, P. D. Rack, and H. Plank, "Direct-write 3D nanoprinting of plasmonic structures," ACS Applied Materials and Interfaces **9**, 8233–8240 (2016).

[10] L. Keller and M. Huth, "Pattern generation for direct-write three-dimensional nanoscale structures via focused electron beam induced deposition," Beilstein Journal of Nanotechnology **9**, 2581–2598 (2018).

[11] M. Pohlit, I. Stockem, F. Porrati, M. Huth, C. Schröder, and J. Müller, "Experimental and theoretical investigation of the magnetization dynamics of an artificial square spin ice cluster," Journal of Applied Physics **120**, 142103 (2016).

[12] M. Pohlit, F. Porrati, M. Huth, Y. Ohno, H. Ohno, and J. Müller, "Magnetic stray-field studies of a single cobalt nanoelement as a component of the building blocks of artificial square spin ice," Journal of Magnetism and Magnetic Materials **400**, 206–212 (2016).

[13] I. Mayergoyz, "Mathematical models of hysteresis," IEEE Transactions on Magnetics **22**, 603–608 (1986).

[14] R. J. Harrison and J. M. Feinberg, "FORCinel: An improved algorithm for calculating first-order reversal curve distributions using locally weighted regression smoothing," Geochemistry, Geophysics, Geosystems **9**, https://doi.org/10.1029/2008gc001987 (2008).

[15] C. Pike and A. Fernandez, "An investigation of magnetic reversal in submicron-scale Co dots using first order reversal curve diagrams," Journal of Applied Physics **85**, 6668–6676 (1999).

[16] C.-I. Dobrotă and A. Stancu, "What does a first-order reversal curve diagram really mean? A study case: Array of ferromagnetic nanowires," Journal of Applied Physics **113**, 043928 (2013).

[17] J. Davies, D. Gilbert, S. M. Mohseni, R. Dumas, J. Åkerman, and K. Liu, "Reversal mode instability and magnetoresistance in perpendicular (Co/Pd)/Cu/(Co/Ni) pseudo-spin-valves," Applied Physics Letters **103**, 022409 (2013).

[18] I. Lascu, J. F. Einsle, M. R. Ball, and R. J. Harrison, "The vortex state in geologic materials: A micromagnetic perspective," Journal of Geophysical Research: Solid Earth **123**, 7285–7304, https://doi.org/10.1029/2018jb015909 (2018).

[19] E. C. Stoner and E. Wohlfarth, "A mechanism of magnetic hysteresis in heterogeneous alloys," Philosophical Transactions of the Royal Society of London. Series A, Mathematical and Physical Sciences **240**, 599–642 (1948).